Presented at 4th International Conference
on Experimental Meson Spectroscopy, Boston,
Massachusetts, April 25-26, 1974

LBL-3010
SLAC PUB No.-1462

AMPLITUDE ANALYSIS OF $(3\pi)^+$ PRODUCTION AT 7 GeV/c

M. Tabak, E. E. Ronat, A. H. Rosenfeld,
T. A. Lasinski and R. J. Cashmore

May 1974

Prepared for the U. S. Atomic Energy Commission
under Contract W-7405-ENG-48

LBL-3010

AMPLITUDE ANALYSIS OF $(3\pi)^+$ PRODUCTION AT 7 GeV/c*

M. Tabak, E. E. Ronat,† A. H. Rosenfeld,
and T. A. Lasinski
Lawrence Berkeley Laboratory
University of California, Berkeley, CA 94720

R. J. Cashmore‡
Stanford Linear Accelerator Center
P. O. Box 4349, Stanford, CA 94305

ABSTRACT

An amplitude analysis of the reaction $\pi^+ p \rightarrow p(\pi^-\pi^+\pi^+)$ at 7 GeV/c is in progress. Although our method of analysis and assumptions are quite different from those of the Illinois group, our preliminary results are nevertheless consistent with theirs. We fit coherent amplitudes, not the density matrix, and make different assumptions about decay amplitudes of J^P states into various isobars. This approach, furthermore, allows us to probe a much larger set of partial waves than that quoted by the Illinois group, at the expense of imposing explicit rank conditions on the density matrix.

I. INTRODUCTION AND FORMALISM

We are pursuing a 3π partial wave analysis of the LBL Group A 7-GeV/c $\pi^+p \rightarrow \pi^+\pi^-\pi^+p$ data.[1] These data have not heretofore been subjected to such analyses. There are two additional new features of the present analysis which should be noted:

1) our formalism and programs have been developed independently of the Illinois effort,[2] and

2) our fitting parameters are associated with amplitudes instead of density matrix elements.

Our formalism[3] and programs have been used in an extensive analysis[4] of the reactions $\pi N \rightarrow \pi\pi N$ in the s-channel resonance region. In spirit, our approach is quite similar to that of the Illinois group.[2] We think of a 3π system with spin J^P and projection M as decaying into an isobar (ϵ, ρ, f) of spin ℓ and a pion with relative orbital angular momentum L. The probability for a given event may be written as

*Work supported in part by the U. S. Atomic Energy Commission.
†Permanent address: Weizmann Inst. of Science, Rehovot, Israel.
‡Now at Oxford University, Oxford, England.

$$P(\text{event}) = \sum_{\eta=\pm 1} \Big\{ \Big| \sum_{\substack{JM \\ L\ell}} A_{++}^{JM\eta L\ell}(M_{3\pi}, t) T_{L\ell}(M_{3\pi}, M_{2\pi}) G^{JM\eta L\ell}(\alpha\beta\gamma\theta_h) \Big|^2$$

$$+ \Big| \sum_{\substack{JM \\ L\ell}} A_{+-}^{JM\eta L\ell}(M_{3\pi}, t) T_{L\ell}(M_{3\pi}, M_{2\pi}) G^{JM\eta L\ell}(\alpha\beta\gamma\theta_h) \Big|^2 \Big\}. \qquad (1)$$

The functions $G^{JM\eta L\ell}$ are essentially the real ($\eta = +1$) and imaginary ($\eta = -1$) parts of $G^{JML\ell}$ given in Ref. 3. The angles $\alpha\beta\gamma$ define an Euler rotation from the production coordinate system (s- or t-channel) to a system with z-axis in the plane of the three pions; θ_h is the helicity decay angle of the isobar. The functions $T_{L\ell}$ are of the form

$$T_{L\ell}(M_{3\pi}, m_{2\pi}) \propto Q^L \, \frac{e^{i\delta_\ell} \sin\delta_\ell}{q^{\ell+1}}, \qquad (2)$$

where δ_ℓ is either approximated by Breit-Wigner behavior or is specified by the actual $\pi\pi$ phase shifts. The discrete quantum number η, which for $M = 0$ is given by

$$\eta = (-1)^{J+L+\ell}, \qquad (3)$$

may be associated with natural and unnatural parity exchange.[5]

Our fitting parameters are the complex "amplitudes"[6] $A^{JM\eta L\ell}$ not density matrix elements. For a given η, we see that for N partial waves there are 4N real parameters to be determined; the corresponding number for a density matrix analysis is N^2. For a given number of fitting parameters, we are thus able to investigate the importance of many more waves than in a density matrix approach. A difficulty associated with an amplitude analysis is the uniqueness of solutions; that is, there are generally several solutions with comparable likelihoods. In view of these remarks, the primary emphasis of the present analysis is to determine which waves are the important ones and to investigate how serious is the ambiguity in solutions.

II. ASSUMPTIONS AND FITTING PROCEDURES

In addition to the isobar assumption implicit in Eq. (1), we have also assumed

1) No $\eta = -1$ waves. Preliminary studies of our data indicate that this approximation is good to about 10%. A notable exception is the A_2 for which $\eta = -1$ contributes about 1/8 to the $J^P = 2^+$ cross section for $M_{3\pi} \approx 1300$ MeV.

2) $A_{+-}^{JML\ell} = 0$. Strictly speaking the assumption[6] here is that of spin-coherence,

$$A_{+-}^{JML\ell} = a\ A_{++}^{JML\ell}, \tag{4}$$

where a is some complex number.

3) Δ^{++} cut, $1160 \leq M_{\pi^+p} \leq 1280$ MeV. The principal effect of this cut is to reduce statistics in the 1600-MeV 3π mass region. No systematic study of the effect of such a cut on our fits has yet been made.

The fitting parameters $A^{JML\ell}$, indexed by $M_{3\pi}$ and t, are determined by likelihood fits to the data. The data were binned into low and high $|t|$ intervals,

$$|t| \leq 0.1\ \mathrm{GeV}^2\ ;\quad 0.1 \leq |t| \leq 0.6\ \mathrm{GeV}^2.$$

The $M_{3\pi}$ binning consisted of nine 100-MeV intervals from 950 to 1750 MeV. For low $|t|$ there were typically 2000 to 700 events per mass bin; for high $|t|$, 2000 to 1500 events per mass bin.

Table I. The waves considered in the present analysis. All waves are $\eta = +1$, $M = 0$ unless otherwise indicated. Double underlined waves were generally "strong"; single underlined waves were considerably "weaker" but definitely present.

	$\rho\pi$	$f\pi$	$\epsilon_{LO}\pi$	$\epsilon_{HI}\pi$
	$\underline{0^- P}$	$0^- D$	$\underline{\underline{0^- S}}$	$0^- S$
(A_1)	$\underline{\underline{1^+ S}}$	$1^+ P$	$1^+ P$	$1^+ P$
	$\underline{1^+ S, M=1}$		$1^+ P, M=1$	$1^+ P, M=1$
	$1^- P, M=1$	$1^- D, M=1$		
	$1^+ D$			
	$\underline{\underline{2^- P}}$	(A_3) $\underline{\underline{2^- S}}$	$\underline{\underline{2^- D}}$	$2^- D$
		$2^- S, M=1$		
(A_2)	$\underline{\underline{2^+ D, M=1}}$	$\underline{2^+ P, M=1}$		
	$\underline{\underline{3^+ D}}$	$3^+ P$	$\underline{\underline{3^+ F}}$	$3^+ F$
	$3^- F, M=1$	$3^- D, M=1$		

The waves included in the present fit are indicated in Table I. The reference wave was taken to be $0^- S \epsilon_{LO} \pi$; that is, in each mass bin we set

$$\mathrm{Im}\, A_{++}^{00S\ \epsilon_{LO}} = 0. \tag{5}$$

Consequently, all phases shown here are measured relative to this wave. The starting parameters for these waves were found through the following procedure. First, we randomly generated in each bin 500 sets of the parameters corresponding to the waves of Table I. We next considered only those 20 sets which had the highest likelihood. Each set was optimized by our fitting program. The net results of this procedure were some 4-17 potential solutions per bin. Depending on the mass bin,[7] these fits involved 43 or 53 parameters.

III. RESULTS FOR LOW MASS (< 1500 MeV)

In Fig. 1 we show the $2^+\rho\pi$ wave for the high $|t|$ interval. Mass, phase, and Argand plots are presented for those solutions which differ by less than 10 points from the highest likelihood solution in each mass bin. The mass and phase plots indicate a rather clean Breit-Wigner-like behavior with mass ~1300 MeV and width ~150 MeV. Note that in the Argand plot (the radius here corresponds to $(\mathrm{events})^{1/2}$) the most rapid motion is between the 1250 and 1350 MeV bins (D and E). The fits for the high $|t|$ data in 50-MeV bins are shown in Fig. 2. The highest likelihood 100-MeV solutions are also indicated with open circles. A similar behavior for the A_2 is also observed at low $|t|$, but only contributes ~60 events out of ~2000 in the 1250-MeV region.

We show our results for the $A_1(\rho\pi)$ in 50- and 100- MeV bins at low and high $|t|$ in Fig. 3. This peak is rather broad, 200-300 MeV, and its position shifts by some 100 MeV between low and high $|t|$. In both cases there is little phase motion, though the high $|t|$ data indicate some small but definite behavior above ~1200 MeV. A better feeling for the significance of this motion is obtained from Fig. 4, where we show the high $|t|$ $A_1(\rho\pi)$ Argand plot. Thus points A through F (925 to 1175 MeV) lie along one radius vector, whereas the higher mass points (G to K) fall off that vector.

For $|t| \leq 0.1$ GeV^2 and $1.0 \leq M_{3\pi} \leq 1.1$ GeV, the linear combinations of $A_1(\rho\pi)$ t-channel density matrix elements corresponding to states of definite η are[5]

$$\rho_{00} = 0.965 \pm 0.086$$

$$\sqrt{2}\ \mathrm{Re}\,\rho_{01} = -0.183 \pm 0.054$$

$$\sqrt{2}\ \mathrm{Im}\,\rho_{01} = 0.005 \pm 0.041$$

$$\rho_{11} - \rho_{1-1} = 0.035 \pm 0.011$$

$$\rho_{11} + \rho_{1-1} = 0\ \text{(Input)}$$

These numbers correspond to the $1^+ \rho\pi$, M=1 wave being present to ~ 3.5σ in our low |t| fits. They are quite similar to those of Ref. 8, keeping in mind the somewhat different |t| and mass intervals.

IV. RESULTS FOR HIGH MASS (> 1500 MeV)

As noted earlier, we have not yet systematically studied the effects of our Δ^{++} cut. In addition, as seen in Fig. 5, there is a definite tendency for our reference wave, $0^- \epsilon_{LO} \pi$, to decrease in the high mass region (1550-1750 MeV). For these reasons we are not prepared as yet to make definite conclusions about phases in this region. With these qualifications in mind, we consider next the principal high-mass waves in our analysis.

A composite of these waves is shown in Fig. 6 for the high |t| region. Notice that the mass region 1550 to 1750 MeV, commonly associated with the A_3, is decomposed in our analysis into six different partial waves: $2^- Sf\pi$, $2^- P\rho\pi$, $2^+ Pf\pi$ (M = 1), $2^- D\epsilon\pi$, $3^+ D\rho\pi$, and $3^+ F\epsilon\pi$. The 3^+ waves are 9 to 10σ effects in our data; the importance of 3^+ has also been observed by a European collaboration.[9] The $2^+ Pf\pi$ is also seen by the CERN-Soviet group,[8] though at a somewhat higher mass and with more intensity.

Our more important waves at low |t| are shown in Fig. 7. Note that the two decay modes for the A_1 ($\rho\pi$ and $\epsilon\pi$) are roughly 90° out of phase. A similar feature is present in the high |t| results. While the 3^+ waves are less striking, it should be noted that "Chew-Low" boundary effects are more severe for the low |t| data.

V. CONCLUSIONS AND PROSPECTUS

The results of the present study may be summarized as follows:

1) The principal waves at low mass (≤ 1500 MeV) are $0^- \epsilon\pi$, $1^+ \rho\pi$, $1^+ \epsilon\pi$, and $2^+ \rho\pi$.

2) The $2^+ \rho\pi$ wave is quite consistent with Breit-Wigner resonance behavior. There is no evidence in the $1^+ \rho\pi, \epsilon\pi$ phases for such an interpretation.

3) Although there are multiple solutions at low mass, they are quantitatively consistent within errors. In addition they are considerably fewer in number than those at high mass.

4) In the A_3 region (1600-1800 MeV), there are at least five important waves present: $2^- f\pi$, $2^- \rho\pi$, $2^- \epsilon\pi$, $3^+ \rho\pi$, $3^+ \epsilon\pi$. Here there are more solutions and they are farther apart than at low mass.

The consistency of our results with those of the Illinois group[2] indicate the viability of an amplitude approach. However, to fully develop this approach, we are pursuing the following projects:

1) Modification of the analysis to measure the eigenvectors of the density matrix. The assumption of spin coherence, while justified by other analyses, clearly deserves independent verification.

2) Development of statistical tests for comparing competing solutions in a given set of partial waves and for selection of the

minimal set of partial waves required by the data. The present criterion, a difference of 10 points in likelihood, is ad hoc.

In the high mass region certain questions independent of our model and peculiar to our data require investigation:

1) How sensitive are the fits to different Δ^{++} cuts?

2) What other choices can be made for reference waves?

The sharp behavior of the $0^-\epsilon\pi$ wave in this region (for high $|t|$) indicates that its use as a reference wave may be unwarranted.

To study the production mechanisms of 3π states, we shall include unnatural parity exchange states in the fits and study more closely the t-dependence of the amplitudes.

REFERENCES

1. M. Alston-Garnjost et al., Phys. Letters 33B, 607 (1970); S. D. Protopopescu et al., Phys. Rev. D 7, 1279 (1973).
2. G. Ascoli et al., Phys. Rev. D 7, 669(1973) and refs. therein. P. V. Brockway, Thesis, U. of Illinois, 1970 (unpublished). J. D. Hansen et al., CERN/D.Ph.II/PHYS 73-34, submitted to Nucl. Phys. B.
3. D. J. Herndon et al., LBL-543 (submitted to Phys. Rev.), 1972.
4. D. J. Herndon et al., LBL-1065 (Rev.), 1974.
5. K. Gottfried and J. D. Jackson, Nuovo Cimento 33, 309 (1964); G. Cohen-Tannondji et al., Nuovo Cimento 55A, 412 (1968); J. P. Ader et al., Nuovo Cimento 56A, 952 (1968).
6. As discussed by Hansen et al. (Ref. 2), we may not in principle uniquely associate A_{++} and A_{+-} with helicity nonflip and flip amplitudes without additional information on the polarization of the protons. This does not, however, invalidate our approach provided additional constraints are imposed on A_{++} and A_{+-} so as to distinguish their contributions in Eq. (1) from the point of view of the fitting program.
7. The waves labeled $\epsilon_{HI}\pi$ were present only in mass bins with $M_{3\pi} > 1200$ MeV. Our ϵ was basically that of the CERN-Munich group, B. Hyams et al., p. 206, $\pi\pi$ Scattering-1973, ed. P. K. Williams and V. Hagopian, AIP, New York, 1973. The distinction between ϵ_{HI} and ϵ_{LO} was as follows:

$$\epsilon_{LO} = \begin{cases} \epsilon_{CM}, & M_{2\pi} \leq 2m_K \\ 0, & M_{2\pi} > 2m_K \end{cases} \qquad \epsilon_{HI} = \begin{cases} 0, & M_{2\pi} < 2m_K \\ \epsilon_{CM}, & M_{2\pi} \geq 2m_K \end{cases} .$$

This division was made to take account of the fact that δ_0^0 passes twice through 90°. For $M_{3\pi} \lesssim 1500$ MeV, the ϵ_{HI} waves contribute no more than ~ 20 events for all solutions. Above this mass these waves are only somewhat larger (~ 30-40 events). There is one solution in the 1650 mass bin which has ~ 100 events in the $2^-\epsilon_{HI}\pi$ wave; we would reject this solution on the basis of continuity in the mass plot.
8. Yu. M. Antipov et al., Nucl. Phys. B63, 141 (1973); B63, 153 (1973).
9. Aachen-Berlin-Bonn-CERN-Heidelberg Coll., CERN/D.Ph.II/PHYS 74.

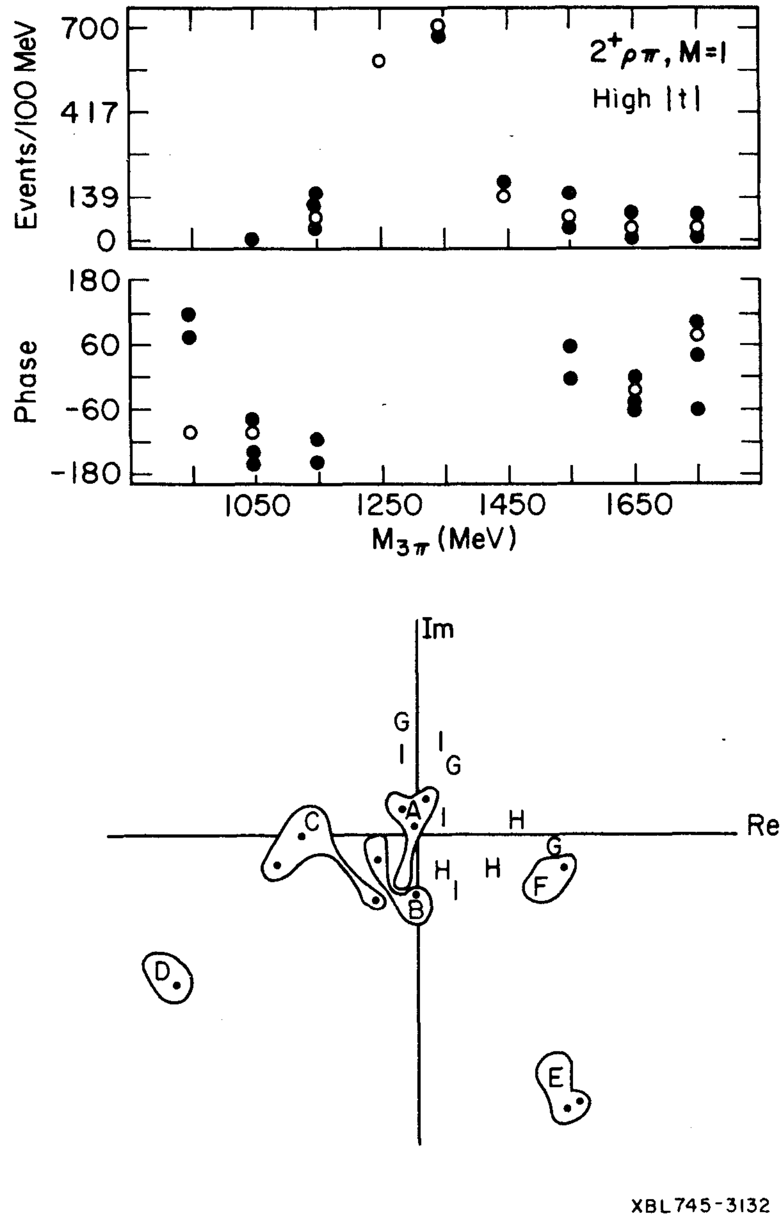

Fig. 1. The A_2 mass, phase and Argand plots for the high | t | interval. Highest likelihood solutions are marked with an open circle in mass and phase plots. In Argand plot they are marked with letters (A = 950 MeV, ···, F = 1450 MeV).

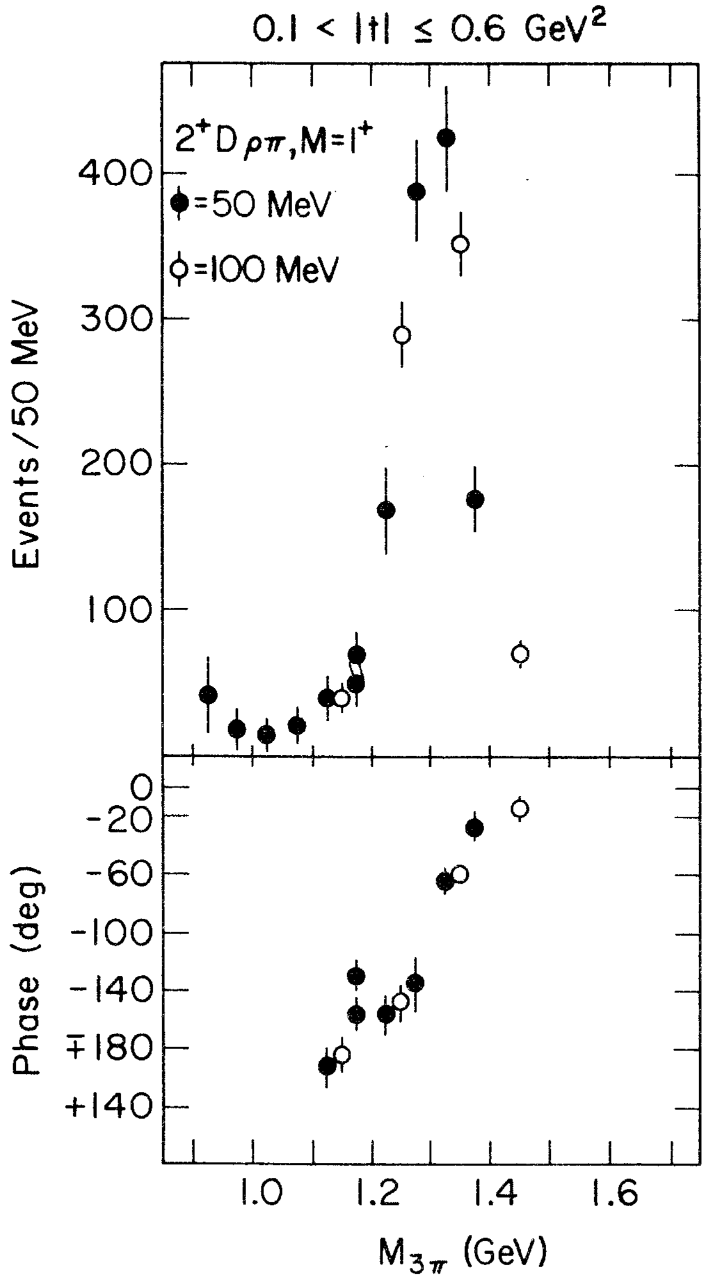

XBL 745-3133

Fig. 2. The A_2 mass and phase plots in 50- and 100-MeV bins for high $|t|$.

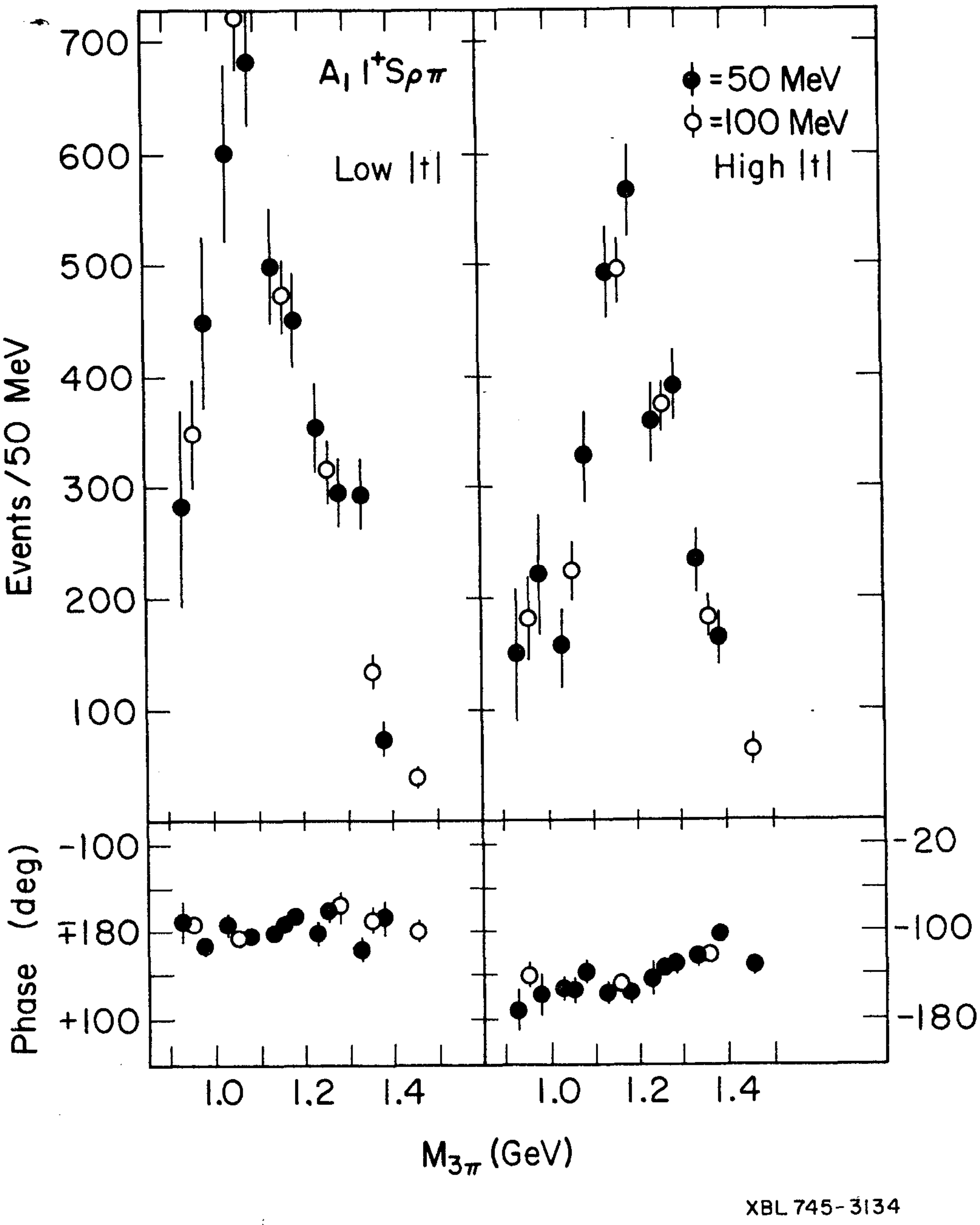

Fig. 3. $1^+\rho\pi(A_1)$ mass and phases plots in 50- and 100-MeV bins for both low and high |t|.

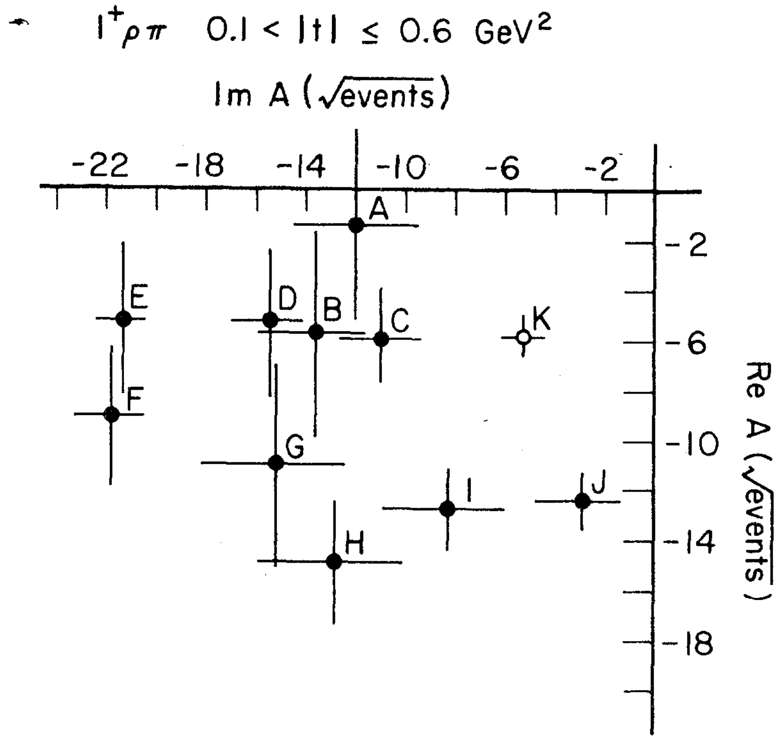

XBL 745-3135

Fig. 4. The A_1 Argand plot for high $|t|$. A = 925, B = 975, ⋯, I = 1325, J = 1375, K = 1450 MeV.

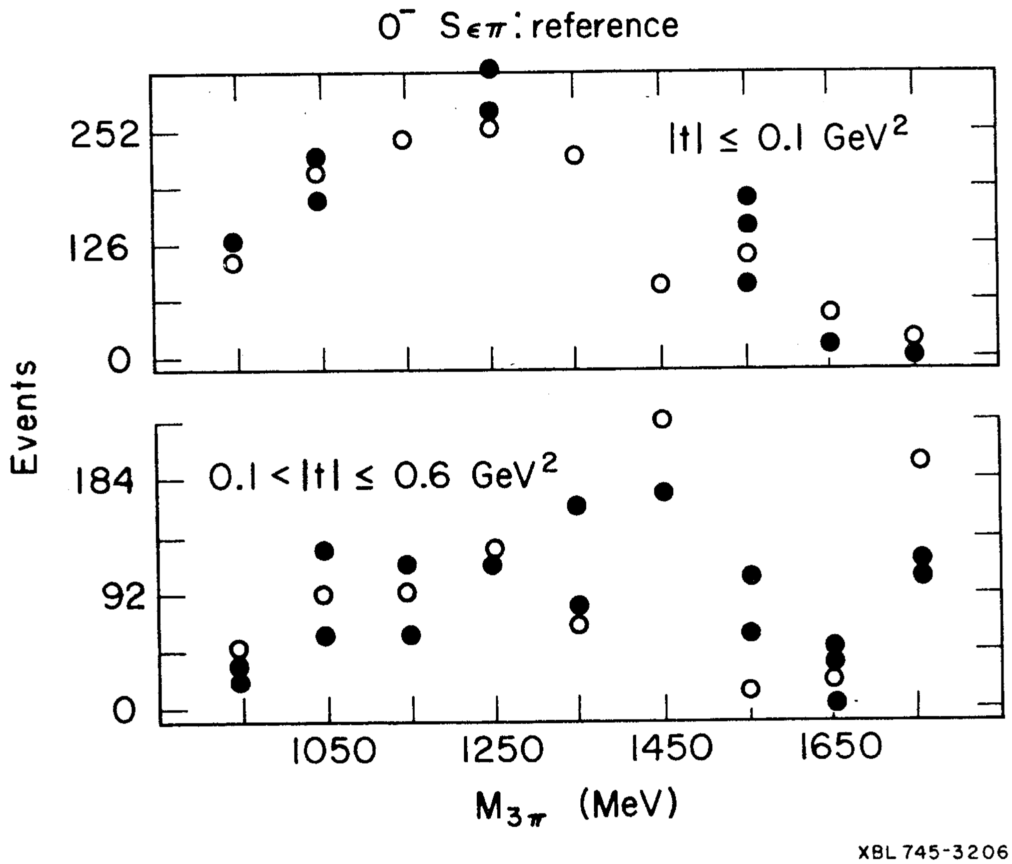

Fig. 5. Mass plots for the reference wave, $0^- \epsilon\pi$, for both low and high $|t|$. The highest likelihood solution in each mass bin is marked by an open circle.

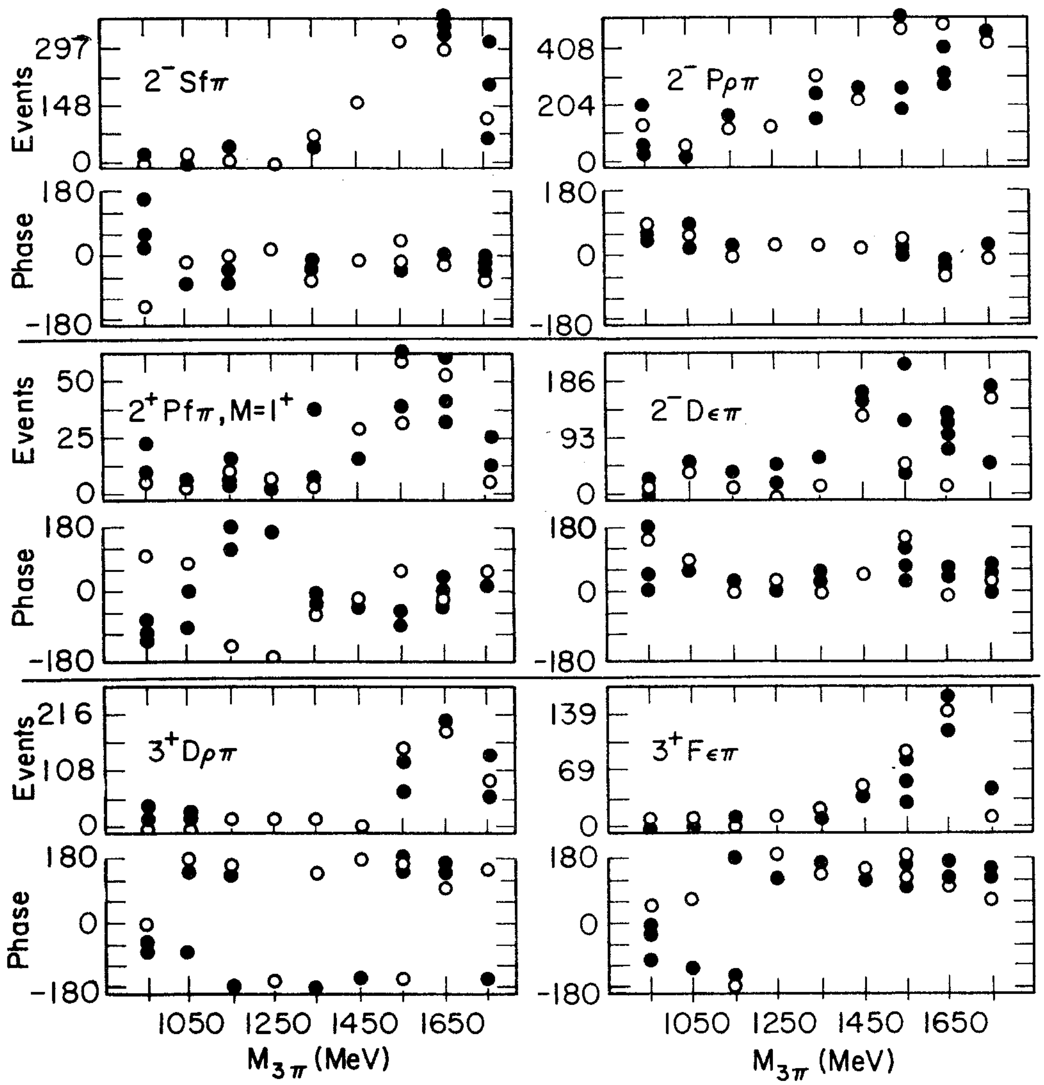

XBL 745-3208

Fig. 6. Additional significant waves for the high |t| interval. An open circle indicates the highest likelihood solution.

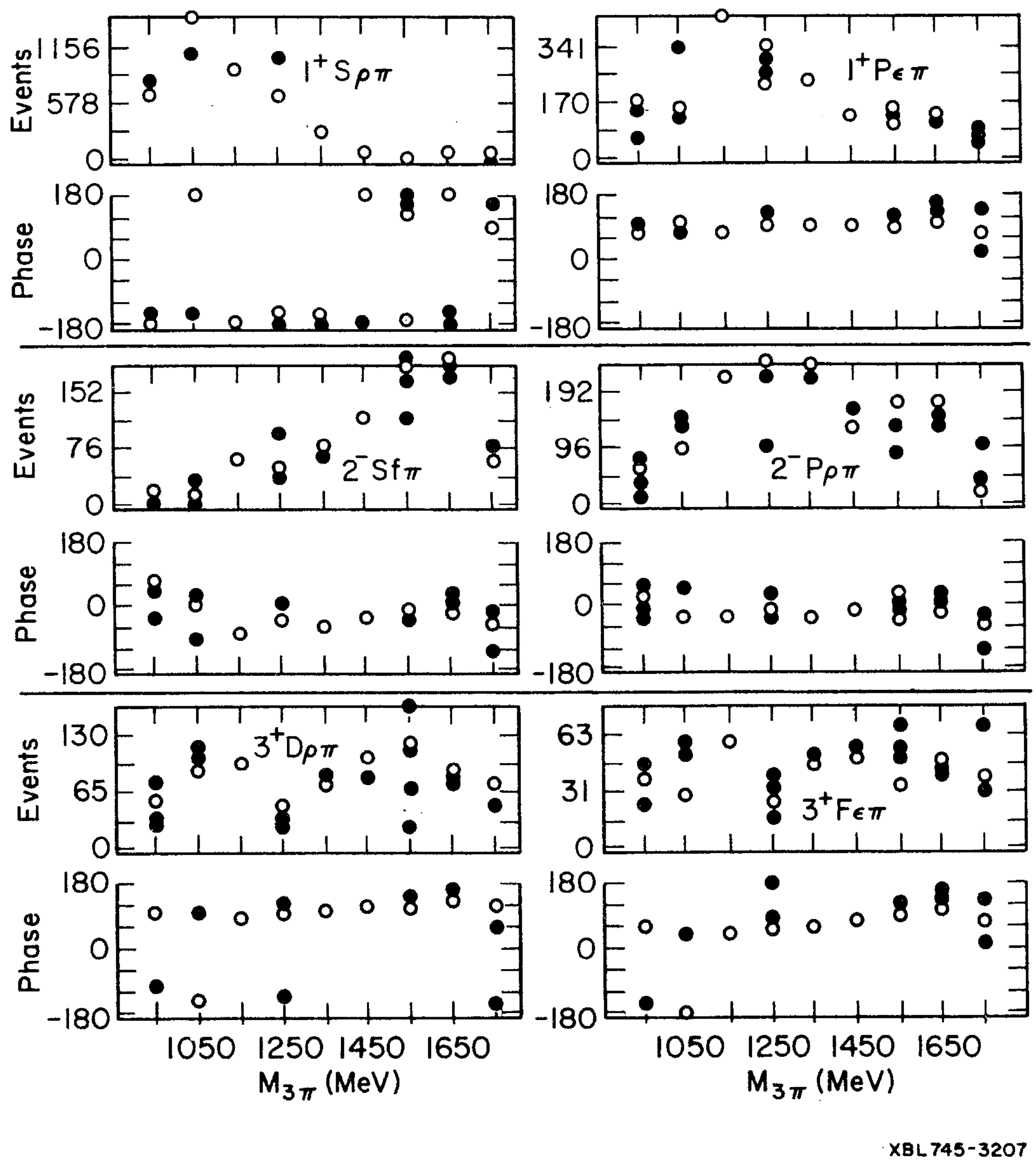

Fig. 7. Important waves for the low |t| interval. An open circle indicates the highest likelihood solution.